Magnetic properties of biogenic selenium nanomaterials

Rewati Dixit[1] · Anirudh Gupta[1] · Norbert Jordan[2] · Shengqiang Zhou[3] · Dieter Schild[4] · Stephan Weiss[2] · Emmanuel Guillon[5] · Rohan Jain[1,6] · Piet Lens[6,7]

Abstract

Bioreduction of selenium oxyanions to elemental selenium is ubiquitous; elucidating the properties of this biogenic elemental selenium (BioSe) is thus important to understand its environmental fate. In this study, the magnetic properties of biogenic elemental selenium nanospheres (BioSe-Nanospheres) and nanorods (BioSe-Nanorods) obtained via the reduction of selenium(IV) using anaerobic granular sludge taken from an upflow anaerobic sludge blanket (UASB) reactor treating paper and pulp wastewater were investigated. The study indicated that the BioSe nanomaterials have a strong paramagnetic contribution with some ferromagnetic component due to the incorporation of Fe(III) (high-spin and low-spin species) as indicated by electron paramagnetic resonance (EPR). The paramagnetism did not saturate up to 50,000 Oe at 5 K, and the hysteresis curve showed the coercivity of 100 Oe and magnetic moment saturation around 10 emu. X-ray photoelectron spectroscopy (XPS) and EPR evidenced the presence of Fe(III) in the nanomaterial. Signals for Fe(II) were observed neither in EPR nor in XPS ruling out its presence in the BioSe nanoparticles. Fe(III) being abundantly present in the sludge likely got entrapped in the extracellular polymeric substances (EPS) coating the biogenic nanomaterials. The presence of Fe(III) in BioSe nanomaterial increases the mobility of Fe(III) and may have an effect on phytoplankton growth in the environment. Furthermore, as supported by the literature, there is a potential to exploit the magnetic properties of BioSe nanomaterials in drug delivery systems as well as in space refrigeration.

Keywords BioSe nanomaterial · Elemental selenium · EPS · Entrapped Fe(III) · Superparamagnetism · Hysteresis curve

Introduction

Selenium (Se) plays an important role in the biochemical cycle of both eukaryotic and prokaryotic organisms due to its presence as a selenocysteine amino acid in many redox-active proteins (Stock and Rother 2009; Kumar et al. 2018). The microbial transformation of Se into its different species affects its bioavailability (Fernández-Martínez and Charlet 2009; Qin et al. 2013). Elemental Se is not bio-available (Wang et al. 2007; Staicu et al. 2015); however, biogenic elemental

Rewati Dixit
dixit.rewati@gmail.com; bez198187@dbeb.iitd.ac.in

Rohan Jain
rohanjain.iitd@gmail.com; rjain@iitd.ac.in

[1] Waste Treatment Laboratory, Department of Biochemical Engineering and Biotechnology, Indian Institute of Technology Delhi, Hauz Khas, New Delhi 110016, India

[2] Helmholtz Zentrum Dresden Rossendorf, Institute of Resource Ecology, Bautzner Landstrasse 400, 01328 Dresden, Germany

[3] Helmholtz Zentrum Dresden Rossendorf, Institute of Ion Beam Physics and Materials Research, Bautzner Landstrasse 400, 01328 Dresden, Germany

[4] Institute for Nuclear Waste Disposal, Karlsruhe Institute of Technology, Hermann von Helmholtz Platz 1, 76344 Eggenstein Leopoldshafen, Germany

[5] Molecular Chemistry Institute of Reims (ICMR UMR CNRS 7312), Environmental Chemistry Group, University of Reims Chamapagne Ardenne, BP 1039, 51687 Reims cedex 2, France

[6] Faculty of Engineering and Natural Sciences, Tampere University of Technology, P.O. Box 1001, FI 33014 Tampere, Finland

[7] UNESCO IHE, Westvest 7, 2611 AX Delft, The Netherlands

selenium (BioSe) nanoparticles are bio-available (Amweg et al. 2003; Li et al. 2014). The microbial transformation of Se oxyanions to elemental Se nanoparticles is omnipresent in the environment (Drewniak and Sklodowska 2013; Jain et al. 2014, 2016; Nancharaiah and Lens 2015; Dessì et al. 2016). Indeed, elemental Se mainly in the form of BioSe nanoparticles can represent 30–60% of the total Se in the sediments, coastal marshes, flow-through wetlands, and aquatic ecosystems (Gao et al. 2000; Zhang et al. 2003; Winkel et al. 2012). Despite the importance of BioSe nanomaterials in understanding the fate of Se, their physical properties are not yet fully deciphered.

The magnetic properties of biominerals play an important role in determining their fate in the environment. For instance, nanoparticles become an integral part of the food web when taken up by plants. Nanoparticles can enter the plants via leaves through the stomatal opening, whereas small quantities are taken up by the lipophilic pathway in the cuticle of leaves or roots through the apoplastic or symplastic pathway (Lv et al. 2019). The magnetic interaction of nanomaterials like Fe_2O_3 makes them accumulate when exposed to high concentrations in plant cells (Shankramma et al. 2016) and soil (Khalilov et al. 2011). In aquatic organisms, the magnetic properties of Fe_3O_4 nanoparticles can alter the toxic dosage, for instance in the case of zebrafish (Malhotra et al. 2019).

Magnetic properties can also be present in non-ferrous biominerals when the iron is naturally doped into them. It has been observed that when ZnO nanoparticles were doped with 1–10% iron by weight, the dissolution of ZnO nanoparticles in the medium was reduced by 14% because of the strong bonding characteristic of Fe(II) in the lattice of ZnO nanoparticles (George et al. 2010). These doped nanoparticles were further tested for toxicity in cell cultures, rat, and zebrafish models. The iron doping reduced the toxic effects of ZnO in vitro as well as in all three in vivo models (Xia et al. 2011). Moreover, magnetotactic bacteria take up Fe from the biosphere and synthesize chains of nanoparticles that act as a magnetic compass (Pradel et al. 2016). It helps them align with the earth's magnetic field to move towards anaerobic zones (Pradel et al. 2016; Schulz-Vogt et al. 2019). Magnetic properties thus influence the fate of biominerals in the environment and are a highly under-investigated property of many biologically produced nanoparticles. No study has so far been carried out to investigate the magnetic properties of BioSe nanomaterials.

The most common treatment for Se-contaminated wastewater is the anaerobic reduction of Se oxyanions leading to the formation of BioSe nanomaterials: BioSe-Nanospheres or BioSe-Nanorods (Lenz et al. 2009; Dessì et al. 2016; Jain et al. 2016). These BioSe nanomaterials are released in the environment, where they interact with plants and microbes. The magnetic properties of one-dimensional chemical Se nanostructures are reported at a temperature below 40 K (Pal et al. 2013). However, the magnetic properties of BioSe nanomaterials have so far not been investigated. In this study, the magnetic properties of BioSe nanomaterial have, therefore, been determined. The presence of iron was detected, and its magnetic properties and oxidation state were analyzed using electron paramagnetic resonance (EPR) and X-ray photoelectron spectroscopy (XPS).

Materials and methods

Production of BioSe-Nanospheres and BioSe-Nanorods

BioSe-Nanospheres and BioSe-Nanorods were produced at 30 °C and 55 °C (Jain et al. 2015a, 2017), respectively, by the reduction of selenite by anaerobic granular sludge procured from a full-scale upflow anaerobic sludge blanket (UASB) reactor treating paper and pulp wastewater (Roest et al. 2005). The elemental Se nanomaterial produced was centrifuged at 3000g and decanted to collect the supernatant. The supernatant was concentrated by high-speed centrifugation at 37,000g followed by sonication. An equal volume of n-hexane was added to the sonicated BioSe nanomaterial. The mixture was left overnight in a separatory funnel, and the BioSe nanomaterial was collected from the aqueous phase. The production and purification method for Se nanoparticles is detailed in earlier studies (Chudobova et al. 2014; Jain et al. 2015a, 2017).

Chemical production of Se nanorods (CheSe-Nanorods)

CheSe-Nanorods were produced by reducing sodium selenite using L-glutathione. L-glutathione and sodium selenite were mixed in a 4:1 ratio. A 6 mol/L of NaOH was added to the mixture to maintain the pH at 7.2 so that the reaction can occur at room temperature (Zhang et al. 2004; Wang et al. 2016).

Magnetic properties of BioSe nanomaterials and CheSe-Nanorods

Magnetic properties were measured by a superconducting quantum interference device (SQUID) magnetometer (Quantum Design, SQUID-VSM). Three kinds of samples, BioSe-Nanorods, BioSe-Nanospheres and CheSe-Nanorods, were measured with the variation of the applied magnetic field (up to 60,000 Oe) and temperature (up to 300 K). The CheSe-Nanorods and the Si substrate used to support the Se nanoparticles were also measured as a reference.

XPS measurements

The uppermost surface layers (up to ~ 10 nm) of the BioSe nanomaterials were analyzed by XPS at room temperature as described by Jain et al. (2015a). Oxidation states were identified by comparison with binding energies reported in the literature (Jain et al. 2015a). Further details are given in the Supporting information (SI).

EPR measurements

EPR spectra were recorded on a Bruker Elexsys 500 EPR spectrometer operating at X-band frequency (9.44 GHz) equipped with a shq0011 cavity fitted with an Oxford instrument liquid helium cryostat operating at 10 K. The following instrument settings were used: field modulation amplitude frequency of 100 kHz, field modulation amplitude of 0.5 mT, a time constant of 0.04 s, sampling time 41 ms, 2048 sampling points, field sweep 0.5 T, and microwave power of 10 mW and 1 mW. One set of BioSe-Nanospheres and BioSe-Nanorods was washed five times with 6 mol/L HCl to remove any surface-bound or loosely bound Fe(III). They were then washed with Milli-Q water (18 MΩ cm) to remove HCl. The amounts of compound dissolved in 1 mL of Milli-Q water introduced in the EPR tubes were the following: BioSe-Nanospheres, 1.6 mg; 6 mol/L HCl–washed BioSe-Nanospheres, 9 mg; BioSe-Nanorods, 1.9 mg, 1 mg; and 6 mol/L HCl–washed BioSe-Nanorods, 18.3 mg.

Easyspin (Stoll and Schweiger 2006) has been used for EPR spectra simulation of the non-saturated experimental spectra after the subtraction of a solvent tube spectrum (or an empty tube). The 'g', D, and (E/D) values are those found to reasonably fit the experimental spectra with the calculated ones using a 'g' strain line-width mode, and 3 to 5 magnetic species in the sample, regarding the relative variation of line intensity at the different microwave power. Details about the parameters are given in the SI.

Results

Magnetic properties of BioSe nanomaterials and CheSe-Nanorods

Both CheSe-Nanorods and Si substrate show a marginal magnetic signal. In sharp contrast, the BioSe-Nanorod sample is
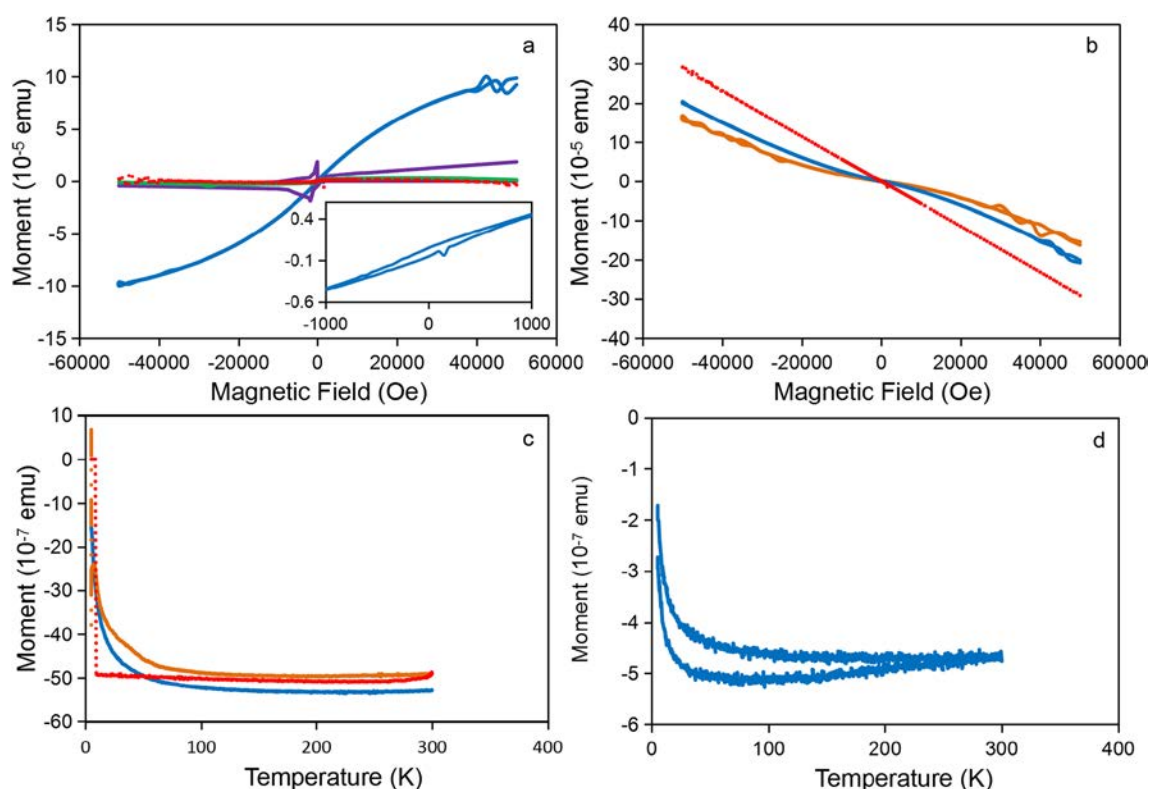

Fig. 1 a Magnetic moment vs. field of BioSe Nanorods after subtraction of the background from the Si supporting substrate with a zoomed in hysteresis curve. b Magnetic moment vs. field of BioSe Nanorods and BioSe Nanospheres measured at 5 K. c Magnetic moment vs. temperature under a field of 1,000 Oe for BioSe Nanospheres and BioSe Nanorods. d Magnetization after zero field cooling (the lower branch) and field cooling (the upper branch) measured under a field of 100 Oe (without subtraction of the background) for BioSe Nanorods. Legends: Blue solid line: BioSe Nanorods large field range; purple long dash: BioSe Nanorods low field range; red round dot: Si substrate reference; green dash: CheSe Nanorods large field range; orange long dash dot dot: BioSe Nanospheres
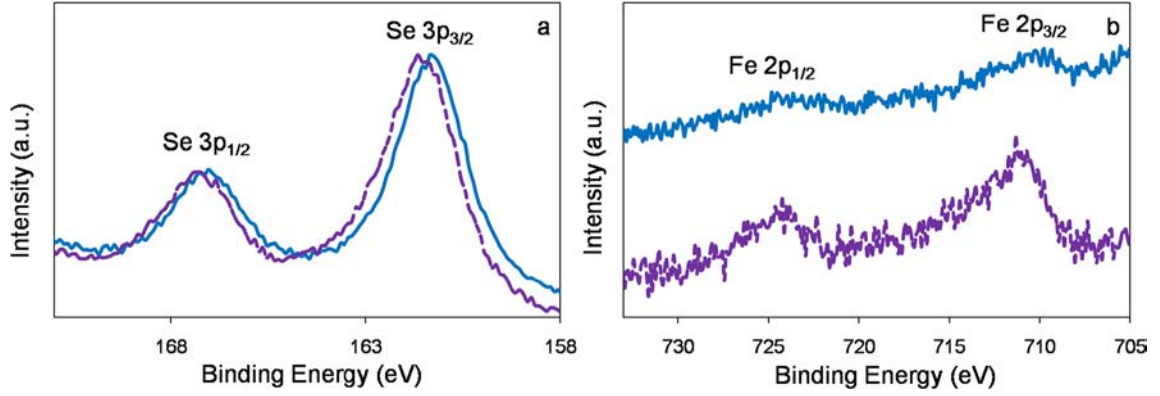
Fig. 2 XP spectra of Se 3p (**a**) and Fe 2p (**b**) elemental lines of BioSe Nanospheres and BioSe Nanorods. Legends: blue solid line: BioSe Nanorods and purple square dot: BioSe Nanospheres

magnetic (Fig. 1a). The large contribution is paramagnetic, but zooming in the low-field part, hysteresis is also resolved as shown in Fig. 1a.

The Si substrate is diamagnetic, which generates a background in all measurements. After subtraction of the diamagnetic signal from the Si substrate, CheSe-Nanorods show only a marginal magnetic signal, while BioSe-Nanorods reveal a large paramagnetic contribution, which does not saturate at magnetic fields up to 50,000 Oe at 5 K (Fig. 1b). In contrast, the CheSe-Nanorod sample does not show a detectable magnetic signal in comparison with the Si-supporting substrate (Fig. 1b).

The paramagnetism in the BioSe-Nanorods can be fitted using the Brillouin function (Coey 2010):

$$M(\alpha) = NJ\mu_B g \left[\frac{2J+1}{2J} \coth\left(\frac{2J+1}{2J}\alpha \right) - \frac{1}{2J}\coth\left(\frac{\alpha}{2J} \right) \right]$$

(1)

where the 'g' factor is assumed to be 2, μ_B is the Bohr magneton, $\alpha = gJ\mu_B H/k_B T$, k_B is the Boltzmann constant, H is the field, T is the temperature and N is the density of spins.

As shown in Fig. 1, the data can be fitted nicely using $J = 5/2$ (Eq. 1). A single paramagnetic center corresponds to $gJ\mu_B = 5 \mu_B$. It is reasonable to attribute the paramagnetic center to

Fe(III) based on earlier studies (Vicente et al. 2016). In consistence, the temperature-dependent magnetization curve can be fitted by the Curie law (Fig. 1c and d) (Wang et al. 2015):

$$\chi = \frac{M}{H} = N\frac{J(J+1)(g\mu_B)^2}{3k_B T}$$

(2)

where M is the magnetic moment per unit volume and H is the magnetizing field intensity.

It is worth noting that the fitting parameters of J and N are the same for Fig. 1a, b, c, and d.

No statistically relevant changes were observed over 3 months in the magnetic properties of BioSe nanomaterials and CheSe-Nanorods (data not shown).

BioSe nanomaterials element analysis using XPS

During the XPS analysis of BioSe nanomaterials, their Se $3p_{3/2}$ binding energy was observed at 161.5 and 161.3 eV for the samples BioSe-Nanospheres and BioSe-Nanorods, respectively (Fig. 2a). This matches well with the binding energy values previously reported in the literature for elemental Se (Jain et al. 2015a).

The formation of BioSe nanomaterials via Se(IV) reduction was revealed by XPS, since no additional peaks at binding
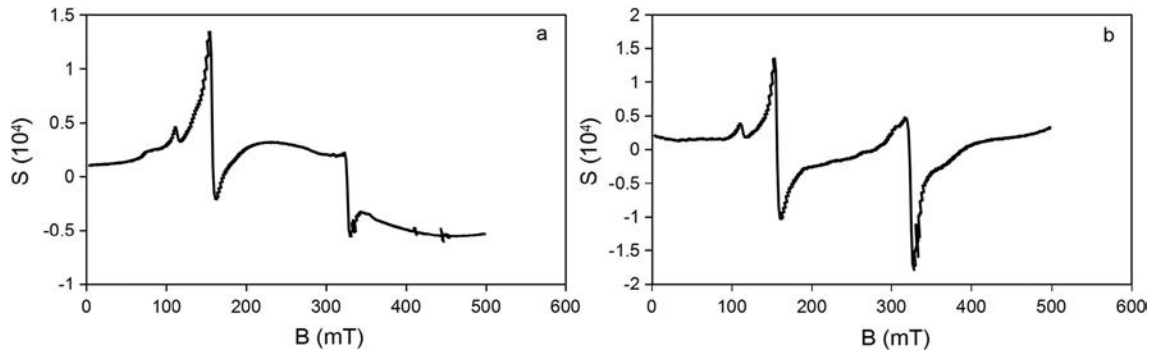

Fig. 3 **a** X band EPR at 10 K of BioSe Nanospheres. **b** X band EPR at 10 K of BioSe Nanorods

Table 1 Paramagnetic species in the BioSe nanomaterials determined using EPR

Samples	Paramagnetic species
BioSe Nanospheres	1. Rhombic high spin Fe(III), 'g' = [9.63 4.27 2.0] (E/D = 0.33)
	2. Axial high spin Fe(III), 'g' = [6.0 2.0] (E/D = 0)
	3. Low spin Fe(III), 'g' = [2.14 2.06 1.84]
	4. Radical », $S = 1/2$, 'g' = 2.011, line width = 0.6 mT
BioSe Nanorods	1. Rhombic high spin Fe(III), 'g' = [9.0 4.27 2.0] (E/D = 0.32)
	2. Axial high spin Fe(III), 'g' = [6.0 2.0] (E/D = 0)
	3. Low spin Fe(III), 'g' = [2.16 2.06 1.81]
	4. Low spin Fe(III), 'g' = [2.22 2.06 2.05]
	5. Radical », $S = 1/2$, 'g' = 2.011, line width = 0.6 mT

energies corresponding to other Se oxidation states were detected (Fig. 2a). The Fe $2p_{3/2}$ binding energy was observed at 711.1 and 710.5 eV for BioSe-Nanospheres and BioSe-Nanorods, respectively (Fig. 2b). The maximum of the Fe $2p_{3/2}$ elemental line in the BioSe-Nanosphere sample suggested the presence of Fe(III), in agreement with former studies (Temesghen and Sherwood 2002; Park et al. 2008). A significant amount of Fe(II) was not observed in Fig. 2b. Indeed, a shoulder at the lower binding energy side of the Fe $2p_{3/2}$ spectrum would have been expected (Huber et al. 2012; Yue et al. 2016). As the iron signal in the XPS spectrum of the BioSe-Nanorods sample was weak, an assignment of the oxidation state of iron was not possible. BioSe-Nanospheres and BioSe-Nanorods exhibited Fe concentrations (at%) of 1.6 and 0.7, respectively. It should be noted that XPS is a surface technique; consequently, the presence of additional iron entrapped inside the BioSe nanomaterial cannot be excluded.

Fe(III) species determination in BioSe nanomaterials using EPR

Rhombic and axial high-spin Fe(III) species with specific 'g' and E/D values were present in the BioSe-Nanosphere spectra (Fig. 3a). The spectrum was also composed of a low-spin Fe(III) species with a specific 'g' value as well as a free radical with a specific spin

quantum number, 'g' value, and line-width. A strong signal of Fe_2O_3 ('g' = 2, 1800 G peak to peak) appears when the temperature reaches 15 K. It is probably due to a superparamagnetic system that is comparable to that of maghemite.

Both rhombic and axial high-spin Fe(III) species with specific 'g' and E/D values were also present in the BioSe-Nanorods spectrum (Fig. 3b and Table 1). Depending on the symmetry of the electronic distribution in different cartesian axes, 'g' can be isotropic ('g'$_x$ = 'g'$_y$ = 'g'$_z$ = 'g'$_{iso}$), axial ('g'$_x$ = 'g'$_y \neq$ 'g'$_z$) or rhombic ('g'$_x \neq$ 'g'$_y \neq$ 'g'$_z$) (Roessler and Salvadori 2018). Thus, rhombic and axial high-spin complexes indicate anisotropic symmetry of the electronic distribution in the molecule. The difference in the 'g' value of a rhombic high-spin complex in BioSe-Nanospheres and BioSe-Nanorods implies a difference in anisotropic symmetry of the electronic distribution of the two nanomaterials (Table 1). The spectrum is also composed of two low-spin Fe(III) species with specific 'g' values as well as a free radical with specific spin density, 'g' value, and line-width.

EPR spectra of high-spin d^5 systems may be interpreted in terms of the spin-Hamiltonian (Mazur et al. 2020):

$$H = \beta H.g.S + D\left(S_z^2 - \frac{35}{12}\right) + E\left(S_x^2 - S_y^2\right) \quad (3)$$

and the ratio of E to D is taken to fall in the range 0–1/3, a value of 0 implying axial symmetry. Each system in Fig. 3

Table 2 Paramagnetic species in the 6 mol/L HCl washed BioSe nanomaterials determined using EPR

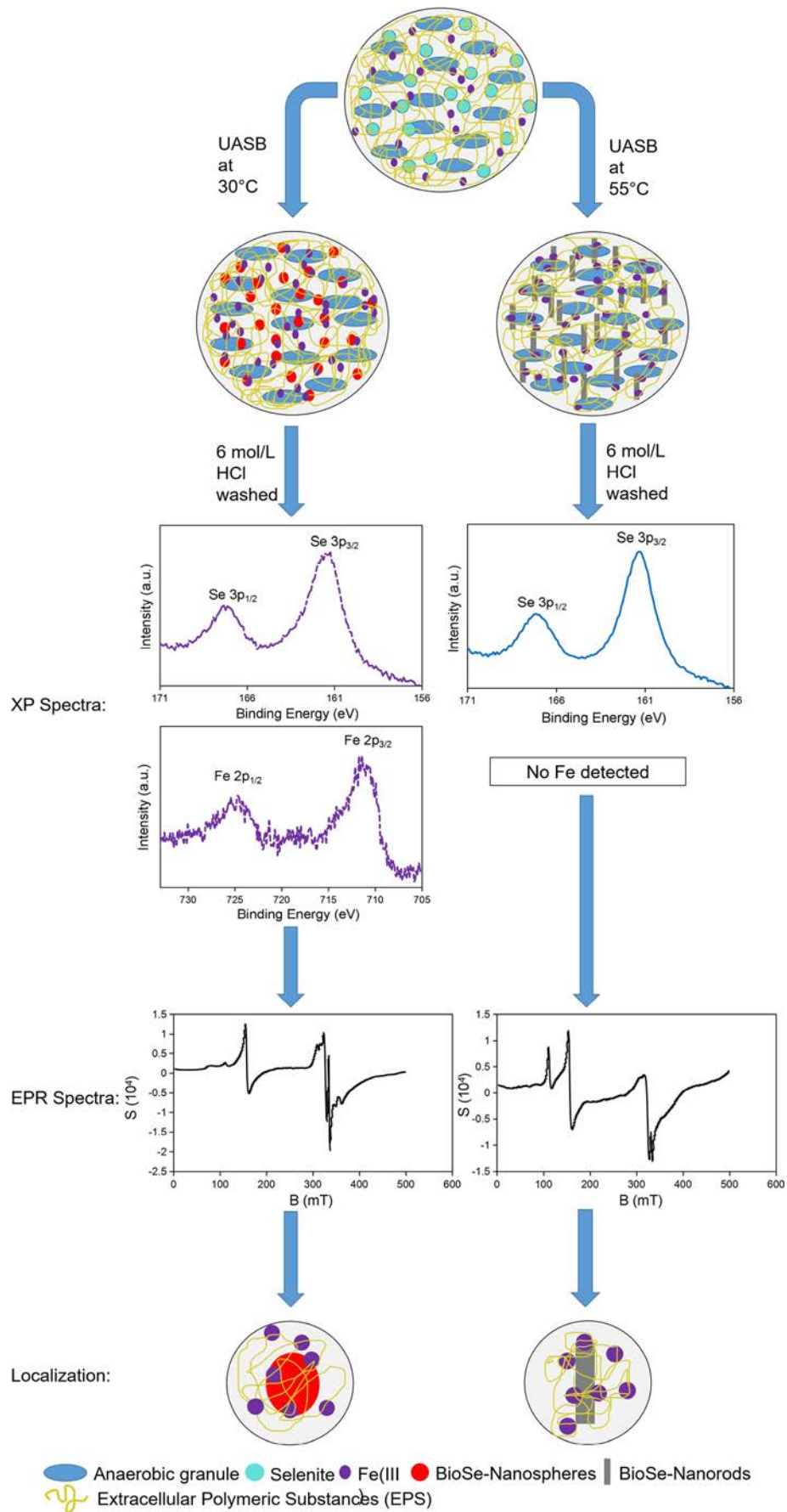| Samples	Paramagnetic species
6 mol/L HCl washed BioSe Nanospheres	1. Rhombic high spin Fe(III), 'g' = [9.0 4.27 2.0] (E/D = 0.33)
	2. Axial high spin Fe(III), 'g' = [6.0 2.0] (E/D = 0)
	3. Low spin Fe(III), 'g' = [2.19 2.06 1.93]
	4. Low spin Fe(III), 'g' = [2.14 2.06 1.84]
	5. Radical », $S = 1/2$, 'g' = 2.011, line width = 0.6 mT
6 mol/L HCl washed BioSe Nanorods	1. Rhombic high spin Fe(III), 'g' = [9.0 4.27 2.0] (E/D = 0.33)
	2. Axial high spin Fe(III), 'g' = [6.0 2.0] (E/D = 0)
	3. Low spin Fe(III), 'g' = [2.48 2.18 1.78]
	4. Low spin Fe(III), 'g' = [2.25 2.07 1.87]
	5. Radical », $S = 1/2$, 'g' = 2.011, line width = 0.3 mT

UASB
at
30°C

UASB
at
55°C

6 mol/L
HCl
washed

6 mol/L
HCl
washed

XP Spectra:

Se 3p$_{1/2}$

Se 3p$_{3/2}$

Intensity (a.u.)

171   166   161   156
Binding Energy (eV)

Se 3p$_{1/2}$

Se 3p$_{3/2}$

Intensity (a.u.)

171   166   161   156
Binding Energy (eV)

Fe 2p$_{1/2}$

Fe 2p$_{3/2}$

Intensity (a.u.)

730   725   720   715   710   705
Binding Energy (eV)

No Fe detected

EPR Spectra:

1.5
1.0
0.5
0
-0.5
-1.0
-1.5
-2.0
-2.5
S (10^4)

0   100   200   300   400   500   600
B (mT)

1.5
1.0
0.5
0
-0.5
-1.0
-1.5
S (10^4)

0   100   200   300   400   500   600
B (mT)

Localization:

Anaerobic granule   Selenite   Fe(III   BioSe-Nanospheres   BioSe-Nanorods
Extracellular Polymeric Substances (EPS)

appears to be a mixture of different Fe(III) species; no Fe(II) species were evidenced. A power saturation study (data not shown) confirmed the presence of these species.

XPS and EPR analysis to determine Fe(III) localization in BioSe nanomaterials

XPS and EPR results show the presence of Fe(III) in both BioSe-Nanospheres and BioSe-Nanorods. This implies that Fe(III) is not merely present on the surface. However, Fe(III) may be loosely bound. Therefore, the nanomaterial was washed 5 times with 6 mol/L HCl to remove loosely bound Fe(III) and analyzed by XPS and EPR. In the XPS analysis, Fe was not detected for 6 mol/L HCl–washed BioSe-Nanorods in contrast to the 6 mol/L HCl–washed BioSe-Nanospheres. Nonetheless, EPR spectra showed the presence of various Fe(III) species in 6 mol/L HCl–washed BioSe-Nanospheres and BioSe-Nanorods as listed in Table 2.

Even after 5 times of washing by HCl (6 mol/L), there was a slight change in the powder spectrum of the BioSe-Nanospheres (Fig. 4). The change was the addition of a low-spin Fe(III) species with a different 'g' value. BioSe-Nanorods when washed 5 times with 6 mol/L HCl (Fig. 4) showed a similar EPR spectrum to non-washed BioSe-Nanorods (Fig. 3b) in terms of high-spin Fe(III) species. There was a change in the low-spin Fe(III) species with respect to the 'g' values. The line-width of the free radical also decreased. When BioSe-Nanorods were washed with HCl, the signal at 'g' = 6 is more important, whereas low-spin components at 'g' = 2 are less important than in the BioSe-Nanospheres after washing with HCl.

Discussion

Fe(III) doping in BioSe nanomaterials

This study demonstrated for the first time that BioSe nanomaterials harbor paramagnetism with some ferromagnetic component in their magnetic properties (Fig. 1). This is due to the doping with Fe(III) which is present in the anaerobic granular sludge used to synthesize the BioSe nanomaterial (Fig. 2). The Fe content of inoculum sludge is typically 20.8–36.0 μg/g TSS (Zandvoort et al. 2006). Fe in granular sludge originates from plumbing, use of fertilizers, or because of Fe-rich industrial wastewater (Vignola et al. 2010). The presence of Fe(III) is likely due to its interaction with extracellular polymeric substances (EPS) which caps the BioSe nanomaterials during their formation (Jain et al. 2015b).

These EPS consist of proteins, humic substances, carbohydrates, and small concentrations of DNA (Jain et al. 2015b) and are a known biosorbent of heavy metal ions (Mohite et al. 2018). Indeed, Fe(III) interacts with various active functional groups present in the EPS, like carboxylic (Tapia et al. 2011), hydroxyl (Tapia et al. 2011), or uronic groups (Sand and Gehrke 2006). The elemental Se when grows into BioSe nanomaterials, the EPS intricately intertwines and incorporates into the nanomaterial (Jain et al. 2015b). Fe(III) being abundantly present in association with the EPS gets incorporated throughout the structure of the nanomaterial and not merely on the surface (Fig. 4). This was evidenced for Fe(III) in a previous study of zinc adsorption (Jain et al. 2015a) on BioSe-Nanospheres using the same anaerobic granular sludge as used in this study. XPS results showed that Fe was present at 5.4 (± 2.5) % w/w of BioSe nanomaterial but the XPS signal was weak; hence, Fe was present entrapped in the nanomaterial (Jain et al. 2015a). Indeed, the detection of Fe(III) by EPR in 6 mol/L HCl–washed BioSe-Nanorods (Fig. 4), when Fe(III) signals were not observed for the same by XPS (Fig. 4), further confirms this finding. Thus, the trapping of Fe(III) in the EPS of BioSe nanomaterials is the cause of the magnetic properties in them.

Another possibility is the existence of Fe(III) forming a covalent bond in the lattice of BioSe nanomaterials. However, considering Fe(III) may not be able to accommodate in a zerovalent uncharged Se(0) structure, there is an unlikelihood of covalent bond formation. This non-covalent bond formation was also observed between Fe(0) and Pd(II) when Pd(II) was doped into Fe(0) nanoparticles (Ling and Zhang 2014).

The magnetic property of the BioSe nanomaterials is weak, and the presence of low-spin species of Fe along with high-spin species causes a reduction in the magnetic moment (Li et al. 2004). Furthermore, low-spin Fe(III) species share electrons rather than occupying orbitals with high energy, whereas the charge distribution becomes more delocalized in high-spin species making them more prone to ionic interactions (Edler and Stein 2014). This property will impact the type of binding of Fe(III) with the EPS functional groups: loosely bound Fe(III) may be removed using HCl washes. However, in this study, HCl treatment led to the appearance of another low-spin species for BioSe-Nanospheres. This might be because HCl washing could not penetrate that close matrix of the Fe–EPS–Se nanomaterials.

Environmental relevance of Fe doping in BioSe nanomaterials

Fe(III) is a regulating component for phytoplankton growth (Fennel et al. 2003). The average total dissolved Fe concentration in the ocean is 0.6–0.7 nmol/L (Hiemstra and van Riemsdijk 2006). The major source of Fe in seawater is the

mixing of Fe-rich sub-surface water (Fennel et al. 2003). Dissolved Fe(III) (bound to humic substances or humic and fulvic acids), when taken up by phytoplankton, increases the chlorophyll concentration and cell yield (Fennel et al. 2003). The deficiency of Fe decreases photosynthetic efficiency (Fennel et al. 2003). Some fraction of the Fe-rich BioSe nanomaterials may remain suspended in the treated water (Tan et al. 2016; Mal et al. 2017) and eventually be released in the sea (Fatoki and Mathabatha 2001). A permissible amount of 5–50 μg/L Se in the effluent is discharged into the freshwater in various nations (Tan et al. 2016). Approximately 1% Fe(III) is present in the BioSe nanomaterials as previously mentioned. This implies that nearly 0.6 nmol/L Fe(III) would be released with these BioSe nanomaterials which is about the same amount of Fe present in the ocean. Though the concentration will get diluted once released into the seawater, the local mixing and local high concentrations of BioSe nanomaterial containing Fe(III) cannot be overlooked (Levasseur et al. 2004). This may lead to increased phytoplankton biomass and a higher carbon export upon the increase of Fe supply (Fennel et al. 2003).

Another aspect of the transfer of Fe to plants is the uptake of BioSe nanomaterials. In general, the major characteristics of nanoparticles that determine plant uptake are size, shape, and surface charge (Lv et al. 2019). It has been demonstrated that 40-nm nanoparticles show 1.8 and 2.2 times higher uptake as compared to 140-nm and 240-nm particle sizes, respectively (Hu et al. 2018). The method of production of nanoparticles is also important for uptake because the BioSe nanoparticles influx (V_{max}) in wheat is 0.76- and 3.3-fold lower than CheSe nanoparticles and selenite, respectively (Hu et al. 2018). However, the transfer of BioSe nanomaterial from the root system to the shoot system in wheat is as low as 0.1 due to retention in roots and rapid conversion to its organic forms. Furthermore, the EPS is mostly hydrophilic (Luna et al. 2014) and could thus facilitate uptake by leaves via the stomatal pathway (Lv et al. 2019). Foliar application of Se nanoparticles on three different onion species resulted in 1.75–4.15 times higher enrichment of Se in plants as compared to selenite application (Golubkina et al. 2012). Se nanoparticles on foliar application also enhanced the antioxidant capacity and biosynthesis of flavonoids in celery by 46.7% and 50.0%, respectively (Li et al. 2020).

Potential applications of Fe(III)-doped BioSe nanomaterials

The hysteresis curve observed for BioSe-Nanorods is attributed to the Fe(III) entrapped in the EPS capping the nanorods (Fig. 1a). The coercivity and magnetic moment associated with Fe(III) in the field of 50,000 Oe are 100 Oe and 10 emu, respectively (Fig. 1a). These low values may be an indication of superparamagnetism (Usov and Liubimov 2012; Ali et al. 2016). Fe(III) nanoparticles in alginate with high magnetism at 5 K and magnetic strength of 5 T have been proposed for controlled drug delivery (Finotelli et al. 2004). The BioSe nanomaterials investigated in this study display similar magnetic characteristics implying a potential for drug delivery. Since Se is known as a good treatment alternative for cancer (Hauksdóttir and Webster 2018), Fe-doped BioSe nanomaterials can be explored. For instance, a study was conducted in which iron oxide nanoparticles decorated with Se were applied to the MB-13 breast cancer cell line. The cells showed a 40.5% reduction in the viability on the first day of the study implying biomedical application (Hauksdóttir and Webster 2018). However, for such purposes, the BioSe nanomaterial needs to be produced under restricted conditions and not from wastewater.

Paramagnetism of magnetic nanomaterials can also be used for magnetic refrigeration (Vlasov et al. 2017). The major working principle behind this is the magnetocaloric effect (MCE). MCE is an inherent property of all magnetic materials. Temperature change is achieved by changing the magnetic field: magnetization reduces entropy, while demagnetization restores zero-field magnetic entropy (Li and Yan 2020). The most important characteristics required for such applications are low magnetic ordering temperature (< 15 K) (Li and Yan 2020) and high spin ($J = 5/2$) (Krastev et al. 2020). Both criteria are met by the BioSe nanomaterial produced in this study. Thus, on a futuristic note, minor doping of Fe(III) in Se nanoparticles with similar magnetic properties like the BioSe nanomaterials investigated in this study may have the potential for space refrigeration.

Conclusion

This is the first study to report that BioSe nanomaterials produced by anaerobic granular sludge taken from a UASB reactor treating paper and pulp wastewater show magnetic properties. Paramagnetism is the major contributor to the magnetic property along with some ferromagnetism. In this study, the BioSe nanomaterial shows paramagnetism at 5 K and does not saturate even at 50,000 Oe, whereas no observable magnetism was observed for CheSe-Nanorods. The Brillouin function fits well for the paramagnetism of BioSe-Nanorods. The magnetism originates from Fe(III) entrapped in the EPS capping the BioSe nanomaterials. The BioSe nanomaterial harbors both high-spin and low-spin species of Fe(III). Fe concentrations (at%) in BioSe-Nanospheres and BioSe-Nanorods are 1.6 and 0.7, respectively. These nanoparticles, when released in the environment, may be taken up by plants and by phytoplankton. This study elaborated on the significance of Fe(III) doping on the magnetic properties of BioSe nanomaterials.

Compliance with ethical standards

Competing interests The authors declare that they have no competing interests.

Ethics approval and consent to participate Not applicable

Consent for publication Not applicable

References

Ali A, Zafar H, Zia M, ul Haq I, Phull AR, Ali JS, Hussain A (2016) Synthesis, characterization, applications, and challenges of iron oxide nanoparticles. Nanotechnol Sci Appl 9:49 67. https://doi.org/10.2147/NSA.S99986

Amweg EL, Stuart DL, Weston DP (2003) Comparative bioavailability of selenium to aquatic organisms after biological treatment of agricultural drainage water. Aquat Toxicol 63:13 25. https://doi.org/10.1016/S0166 445X(02)00110 8

Chudobova D, Cihalova K, Dostalova S, Ruttkay Nedecky B, Merlos Rodrigo MA, Tmejova K, Kopel P, Nejdl L, Kudr J, Gumulec J, Krizkova S, Kynicky J, Kizek R, Adam V (2014) Comparison of the effects of silver phosphate and selenium nanoparticles on *Staphylococcus aureus* growth reveals potential for selenium particles to prevent infection. FEMS Microbiol Lett 351:195 201. https://doi.org/10.1111/1574 6968.12353

Coey JMD (2010) Magnetism and magnetic materials. Cambridge University Press, Cambridge

Dessì P, Jain R, Singh S, Seder Colomina M, van Hullebusch ED, Rene ER, Ahammad SZ, Carucci A, Lens PNL (2016) Effect of temperature on selenium removal from wastewater by UASB reactors. Water Res 94:146 154. https://doi.org/10.1016/j.watres.2016.02.007

Drewniak L, Sklodowska A (2013) Arsenic transforming microbes and their role in biomining processes. Environ Sci Pollut Res 20:7728 7739. https://doi.org/10.1007/s11356 012 1449 0

Edler E, Stein M (2014) Spin state dependent properties of an iron(III) hydrogenase mimic. Eur J Inorg Chem 2014:3587 3599. https://doi.org/10.1002/ejic.201402295

Fatoki OS, Mathabatha S (2001) An assessment of heavy metal pollution in the East London and Port Elizabeth harbours. Water SA 27:233 240. https://doi.org/10.4314/wsa.v27i2.4997

Fennel K, Abbott MR, Spitz YH, Richman JG, Nelson DM (2003) Impacts of iron control on phytoplankton production in the modern and glacial Southern Ocean. Deep Res Part II Top Stud Oceanogr 50:833 851. https://doi.org/10.1016/S0967 0645(02)00596 9

Fernández Martínez A, Charlet L (2009) Selenium environmental cycling and bioavailability: a structural chemist point of view. Rev Environ Sci Biotechnol 8:81 110. https://doi.org/10.1007/s11157 009 9145 3

Finotelli PV, Morales MA, Rocha Leão MH, Baggio Saitovitch EM, Rossi AM (2004) Magnetic studies of iron(III) nanoparticles in alginate polymer for drug delivery applications. Mater Sci Eng C 24:625 629. https://doi.org/10.1016/j.msec.2004.08.005

Gao S, Tanji KK, Peters DW, Herbel MJ (2000) Water selenium speciation and sediment fractionation in a California flow through wetland system. J Environ Qual 29:1275 1283. https://doi.org/10.2134/jeq2000.00472425002900040034x

George S, Pokhrel S, Xia T, Gilbert B, Ji Z, Schowalter M, Rosenauer A, Damoiseaux R, Bradley KA, Mädler L, Nel AE (2010) Use of a rapid cytotoxicity screening approach to engineer a safer zinc oxide nanoparticle through iron doping. ACS Nano 4:15 29. https://doi.org/10.1021/nn901503q

Golubkina NA, Folmanis GE, Tananaev IG (2012) Comparative evaluation of selenium accumulation by *Allium* species after foliar application of selenium nanoparticles, sodium selenite and sodium selenate. Dokl Biol Sci 444:176 179. https://doi.org/10.1134/S0012496612030076

Hauksdóttir HL, Webster TJ (2018) Selenium and iron oxide nanocomposites for magnetically targeted anti cancer applications. J Biomed Nanotechnol 14:510 525. https://doi.org/10.1166/jbn 2018.2521

Hiemstra T, van Riemsdijk WH (2006) Biogeochemical speciation of Fe in ocean water. Mar Chem 102:181 197. https://doi.org/10.1016/j.marchem.2006.03.008

Hu T, Li H, Li J, Zhao G, Wu W, Liu L, Wang Q, Guo Y (2018) Absorption and bio transformation of selenium nanoparticles by wheat seedlings (*Triticumaestivum L.*). Front. Plant Sci 9:597. https://doi.org/10.3389/fpls.2018.00597

Huber F, Schild D, Vitova T, Rothe J, Kirsch R, Schäfer T (2012) U(VI) removal kinetics in presence of synthetic magnetite nanoparticles. Geochim Cosmochim Acta 96:154 173. https://doi.org/10.1016/j.gca.2012.07.019

Jain R, Gonzale Gil G, Singh V et al (2014) Biogenic selenium nanoparticles: production, characterization and challenges. In: Biotechnology Volume 10: Nanobiotechnology, Studium Press LLC, pp 365 394

Jain R, Jordan N, Schild D, van Hullebusch ED, Weiss S, Franzen C, Farges F, Hübner R, Lens PNL (2015a) Adsorption of zinc by biogenic elemental selenium nanoparticles. Chem Eng J 260:855 863. https://doi.org/10.1016/j.cej.2014.09.057

Jain R, Jordan N, Weiss S, Foerstendorf H, Heim K, Kacker R, Hübner R, Kramer H, van Hullebusch ED, Farges F, Lens PNL (2015b) Extracellular polymeric substances govern the surface charge of biogenic elemental selenium nanoparticles. Environ Sci Technol 49:1713 1720. https://doi.org/10.1021/es5043063

Jain R, Matassa S, Singh S, van Hullebusch ED, Esposito G, Lens PNL (2016) Reduction of selenite to elemental selenium nanoparticles by activated sludge. Environ Sci Pollut Res 23:1193 1202. https://doi.org/10.1007/s11356 015 5138 7

Jain R, Jordan N, Tsushima S, Hübner R, Weiss S, Lens PNL (2017) Shape change of biogenic elemental selenium nanomaterials from

nanospheres to nanorods decreases their colloidal stability. Environ Sci Nano 4:1054 1063. https://doi.org/10.1039/c7en00145b

Khalilov RI, Nasibova AN, Serezhenkov VA, Ramazanov MA, Kerimov MK, Garibov AA, Vanin AF (2011) Accumulation of magnetic nanoparticles in plants grown on soils of Apsheron peninsula. Biophysics (Oxf) 56:316 322. https://doi.org/10.1134/S000635091102014X

Krastev PB, Gunnlaugsson HP, Nomura K, Bharuth Ram K, Qi B, Masenda H, Mølholt TE, Naidoo D, Ólafsson S, Martín Luengo AT, Unzueta I, Johnston K, Schell J, Gislason HP (2020) Local increase of the Curie temperature in Mn/Fe implanted $Y_3Fe_5O_{12}$ (YIG). Appl Radiat Isot 160:2 6. https://doi.org/10.1016/j.apradiso.2020.109121

Kumar N, Krishnani KK, Singh NP (2018) Comparative study of selenium and selenium nanoparticles with reference to acute toxicity, biochemical attributes, and histopathological response in fish. Environ Sci Pollut Res 25:8914 8927. https://doi.org/10.1007/s11356 017 1165 x

Lenz M, Enright AM, O'Flaherty V, van Aelst AC, Lens PNL (2009) Bioaugmentation of UASB reactors with immobilized *Sulfurospirillum barnesii* for simultaneous selenate and nitrate removal. Appl Microbiol Biotechnol 83:377 388. https://doi.org/10.1007/s00253 009 1915 x

Levasseur S, Frank M, Hein JR, Halliday AN (2004) The global variation in the iron isotope composition of marine hydrogenetic ferromanganese deposits: Implications for seawater chemistry? Earth Planet Sci Lett 224:91 105. https://doi.org/10.1016/j.epsl.2004.05.010

Li L, Yan M (2020) Recent progresses in exploring the rare earth based intermetallic compounds for cryogenic magnetic refrigeration. J Alloys Compd 823:153810. https://doi.org/10.1016/j.jallcom.2020.153810

Li J, Struzhkin VV, Mao HK, Shu J, Hemley RJ, Fei Y, Mysen B, Dera P, Prakapenka V, Shen G (2004) Electronic spin state of iron in lower mantle perovskite. Proc Natl Acad Sci U S A 101:14027 14030. https://doi.org/10.1073/pnas.0405804101

Li DB, Cheng YY, Wu C, Li WW, Li N, Yang ZC, Tong ZH, Yu HQ (2014) Selenite reduction by *Shewanella oneidensis* MR 1 is mediated by fumarate reductase in periplasm. Sci Rep 4:1 7. https://doi.org/10.1038/srep03735

Li D, An Q, Wu Y, Li JQ, Pan C (2020) Foliar application of selenium nanoparticles on celery stimulates several nutrient component levels by regulating the α linolenic acid pathway. ACS Sustain Chem Eng 8:10502 10510. https://doi.org/10.1021/acssuschemeng.0c02819

Ling L, Zhang WX (2014) Structures of Pd Fe(0) bimetallic nanoparticles near 0.1 nm resolution. RSC Adv 4:33861 33865. https://doi.org/10.1039/c4ra04311a

Luna H, Baêta B, Aquino S, Rodríguez Susa M (2014) EPS and SMP dynamics at different heights of a submerged anaerobic membrane bioreactor (SAMBR). Process Biochem 49:2241 2248. https://doi.org/10.1016/j.procbio.2014.09.013

Lv J, Christie P, Zhang S (2019) Uptake, translocation, and transformation of metal based nanoparticles in plants: recent advances and methodological challenges. Environ Sci Nano 6:41 59. https://doi.org/10.1039/C8EN00645H

Mal J, Veneman WJ, Nancharaiah YV, van Hullebusch ED, Peijnenburg WJGM, Vijver MG, Lens PNL (2017) A comparison of fate and toxicity of selenite, biogenically, and chemically synthesized selenium nanoparticles to zebrafish (*Danio rerio*) embryogenesis. Nanotoxicology 11:87 97. https://doi.org/10.1080/17435390.2016.1275866

Malhotra N, Chen JR, Sarasamma S, Audira G, Siregar P, Liang ST, Lai YH, Lin GM, Ger TR, Hsiao CD (2019) Ecotoxicity assessment of Fe_3O_4 magnetic nanoparticle exposure in adult zebrafish at an environmental pertinent concentration by behavioral and biochemical testing. Nanomaterials 9:873. https://doi.org/10.3390/nano9060873

Mazur M, Pogány L, Brachňaková B, Šalitroš I (2020) A variable temperature Q and X band EPR study of spin crossover iron(III) Schiff base complex. Chem Pap 74:3683 3692. https://doi.org/10.1007/s11696 019 00781 2

Mohite BV, Koli SH, Patil SV (2018) Heavy metal stress and its consequences on exopolysaccharide (EPS) producing *Pantoea agglomerans*. Appl Biochem Biotechnol 186:199 216. https://doi.org/10.1007/s12010 018 2727 1

Nancharaiah YV, Lens PNL (2015) Ecology and biotechnology of selenium respiring bacteria. Microbiol Mol Biol Rev 79:61 80. https://doi.org/10.1128/mmbr.00037 14

Pal A, Shirodkar SN, Gohil S, Ghosh S, Waghmare UV, Ayyub P (2013) Multiferroic behavior in elemental selenium below 40 K: effect of electronic topology. Sci Rep 3:1 7. https://doi.org/10.1038/srep02051

Park H, Ayala P, Deshusses MA et al (2008) Electrodeposition of maghemite (γ Fe_2O_3) nanoparticles. Chem Eng J 139:208 212. https://doi.org/10.1016/j.cej.2007.10.025

Pradel N, Fuduche M, Ollivier B (2016) Magnetotactic bacteria population in a pristine French Atlantic lagoon. Environ Sci Pollut Res 23:691 697. https://doi.org/10.1007/s11356 015 5322 9

Qin T, Chen J, Wang D, Hu Y, Zhang J, Wang M, Qiu S, Gao Z, liu R, Yu Y, Huang Y, Wang Q, Wang Q (2013) Selenylation modification can enhance immune enhancing activity of Chinese angelica polysaccharide. Carbohydr Polym 95:183 187. https://doi.org/10.1016/j.carbpol.2013.02.072

Roessler MM, Salvadori E (2018) Principles and applications of EPR spectroscopy in the chemical sciences. Chem Soc Rev 47:2534 2553. https://doi.org/10.1039/c6cs00565a

Roest K, Heilig HGHJ, Smidt H, de Vos WM, Stams AJM, Akkermans ADL (2005) Community analysis of a full scale anaerobic bioreactor treating paper mill wastewater. Syst Appl Microbiol 28:175 185. https://doi.org/10.1016/j.syapm.2004.10.006

Sand W, Gehrke T (2006) Extracellular polymeric substances mediate bioleaching/biocorrosion via interfacial processes involving iron(III) ions and acidophilic bacteria. Res Microbiol 157:49 56. https://doi.org/10.1016/j.resmic.2005.07.012

Schulz Vogt HN, Pollehne F, Jürgens K, Arz HW, Beier S, Bahlo R, Dellwig O, Henkel JV, Herlemann DPR, Krüger S, Leipe T, Schott T (2019) Effect of large magnetotactic bacteria with polyphosphate inclusions on the phosphate profile of the suboxic zone in the Black Sea. ISME J 13:1198 1208. https://doi.org/10.1038/s41396 018 0315 6

Shankramma K, Yallappa S, Shivanna MB, Manjanna J (2016) Fe_2O_3 magnetic nanoparticles to enhance *S. lycopersicum* (tomato) plant growth and their biomineralization. Appl Nanosci 6:983 990. https://doi.org/10.1007/s13204 015 0510 y

Staicu LC, van Hullebusch ED, Lens PNL, Pilon Smits EAH, Oturan MA (2015) Electrocoagulation of colloidal biogenic selenium. Environ Sci Pollut Res 22:3127 3137. https://doi.org/10.1007/s11356 014 3592 2

Stock T, Rother M (2009) Selenoproteins in Archaea and Gram positive bacteria. Biochim Biophys Acta, Gen Subj 1790:1520 1532. https://doi.org/10.1016/j.bbagen.2009.03.022

Stoll S, Schweiger A (2006) EasySpin, a comprehensive software package for spectral simulation and analysis in EPR. J Magn Reson 178:42 55. https://doi.org/10.1016/j.jmr.2005.08.013

Tan LC, Nancharaiah YV, van Hullebusch ED, Lens PNL (2016) Selenium: environmental significance, pollution, and biological treatment technologies. Biotechnol Adv 34:886 907. https://doi.org/10.1016/j.biotechadv.2016.05.005

Tapia JM, Muñoz JA, González F, Blázquez ML, Ballester A (2011) Mechanism of adsorption of ferric iron by extracellular polymeric substances (EPS) from a bacterium *Acidiphilium* sp. Water Sci Technol 64:1716 1722. https://doi.org/10.2166/wst.2011.649

Temesghen W, Sherwood PMA (2002) Analytical utility of valence band X ray photoelectron spectroscopy of iron and its oxides, with spec tral interpretation by cluster and band structure calculations. Anal Bioanal Chem 373:601 608. https://doi.org/10.1007/s00216 002 1362 3

Usov NA, Liubimov BY (2012) Dynamics of magnetic nanoparticle in a viscous liquid: application to magnetic nanoparticle hyperthermia. J Appl Phys 112:02. https://doi.org/10.1063/1.4737126

Vicente AI, Joseph A, Ferreira LP, de Deus Carvalho M, Rodrigues VHN, Duttine M, Diogo HP, Minas da Piedade ME, Calhorda MJ, Martinho PN (2016) Dynamic spin interchange in a tridentate Fe(III) Schiff base compound. Chem Sci 7:4251 4258. https://doi.org/10.1039/c5sc04577k

Vignola F, Borges DLG, Curtius AJ, Welz B, Becker Ross H (2010) Simultaneous determination of Cd and Fe in sewage sludge by high resolution continuum source electrothermal atomic absorption spectrometry with slurry sampling. Microchem J 95:333 336. https://doi.org/10.1016/j.microc.2010.01.014

Vlasov A, Guillemette J, Gervais G, Szkopek T (2017) Magnetic refrig eration with paramagnetic semiconductors at cryogenic tempera tures. Appl Phys Lett 111:14. https://doi.org/10.1063/1.4994536

Wang H, Zhang J, Yu H (2007) Elemental selenium at nano size pos sesses lower toxicity without compromising the fundamental effect on selenoenzymes: Comparison with selenomethionine in mice. Free Radic Biol Med 42:1524 1533. https://doi.org/10.1016/j.freeradbiomed.2007.02.013

Wang Y, Liu Y, Wendler E, Hübner R, Anwand W, Wang G, Chen X, Tong W, Yang Z, Munnik F, Bukalis G, Chen X, Gemming S, Helm M, Zhou S (2015) Defect induced magnetism in SiC: interplay be tween ferromagnetism and paramagnetism. Phys Rev B Condens Matter Mater Phys 92:1 11. https://doi.org/10.1103/PhysRevB.92.174409

Wang Q, Mejía Jaramillo A, Pavon JJ, Webster TJ (2016) Red selenium nanoparticles and gray selenium nanorods as antibacterial coatings for PEEK medical devices. J Biomed Mater Res Part B Appl Biomater 104:1352 1358. https://doi.org/10.1002/jbm.b.33479

Winkel LHE, Johnson CA, Lenz M, Grundl T, Leupin OX, Amini M, Charlet L (2012) Environmental selenium research: from micro scopic processes to global understanding. Environ Sci Technol 46:571 579. https://doi.org/10.1021/es203434d

Xia T, Zhao Y, Sager T, George S, Pokhrel S, Li N, Schoenfeld D, Meng H, Lin S, Wang X, Wang M, Ji Z, Zink JI, Mädler L, Castranova V, Lin S, Nel AE (2011) Decreased dissolution of ZnO by iron doping yields nanoparticles with reduced toxicity in the rodent lung and zebrafish embryos. ACS Nano 5:1223 1235. https://doi.org/10.1021/nn1028482

Yue X, Guo W, Li X, Zhou H, Wang R (2016) Core shell Fe_3O_4@MIL 101(Fe) composites as heterogeneous catalysts of persulfate activa tion for the removal of Acid Orange 7. Environ Sci Pollut Res 23:15218 15226. https://doi.org/10.1007/s11356 016 6702 5

Zandvoort MH, van Hullebusch ED, Gieteling J, Lens PNL (2006) Granular sludge in full scale anaerobic bioreactors: trace element content and deficiencies. Enzym Microb Technol 39:337 346. https://doi.org/10.1016/j.enzmictec.2006.03.034

Zhang Y, Zahir ZA, Frankenberger WT (2003) Factors affecting reduc tion of selenate to elemental selenium in agricultural drainage water by *Enterobacter taylorae*. J Agric Food Chem 51:7073 7078. https://doi.org/10.1021/jf0304019

Zhang J, Wang H, Bao Y, Zhang L (2004) Nano red elemental selenium has no size effect in the induction of seleno enzymes in both cul tured cells and mice. Life Sci 75:237 244. https://doi.org/10.1016/j.lfs.2004.02.004